ANL-HEP-TR--91-62

DE91 018892

The effect of passive material on the detection of hadrons in calorimeter configurations for the SDC detector*

THOMAS B. W. KIRK AND HANS-JOCHEN TROST

High Energy Physics Division - 362 -
Argonne National Laboratory
9700 S. Cass Ave., Argonne, IL 60439-4815, USA

14 August 1991

ABSTRACT

We have used a flexible geometry model of a calorimeter design for SDC to study the effect of passive material in front of the calorimeter and between the barrel and endcap modules on the apparent response to hadrons. The thicknesses of the passive materials have been chosen to closely resemble the currently projected wall thicknesses of the scintillating tile-fiber and liquid-argon calorimeter designs. The liquid-argon model contains about three times the amount of material in its shells compared to the tile-fiber model. The solenoid coil reduces the relative difference somewhat in the barrel region but constitutes only a minor correction in the transition region from barrel to endcap. Correspondingly, we find a significantly worse response for the liquid-argon case which we demonstrate using beams of single π^- particles of 10 GeV/c momentum.

* Work supported by the U.S. Department of Energy, Division of High Energy Physics, Contract W-31-109-ENG-38

1. Introduction

Two technological options for the main calorimeter of the SDC detector[1] are currently being considered, a scintillator sandwich calorimeter using lead and iron as absorbers, and a liquid-argon calorimeter with lead absorbers. The effect of passive material in front of calorimeters and around them has been of great concern for some time.[2–4] After the mechanical designs for the SDC calorimeter options are becoming quite detailed and solid now, we decided to use the ANLSIM simulation program[5] with a flexible geometry model[6] to study the effect of the solenoidal coil and calorimeter shell materials combined on the response of the calorimeter to hadrons.

2. Detector setups for the simulation

The use of the existing program[5,6] "as is" has some implications on the actual representation of the detectors in the program. First, the active calorimeter medium is a homogeneous representation of a ZEUS style calorimeter made of 3.3 *mm* thick uranium plates and 2.6 *mm* thick scintillator tiles while both SDC design in question are based on lead as the absorber material. The passive material can only be included in the coil and a side support cone of the barrel calorimeter, and is is bound to be aluminium. Thus we will convert the steel shells of the SDC scintillator calorimeter to equivalent aluminium shells as described below. We want to emphasize here that the use of a uranium-scintillator model for the active calorimetry regions does give resolutions comparable to those achieved both with lead-scintillator[7] and lead-liquid-argon calorimeters[8] (with copper or iron in the hadronic sections, maintaining the effective interaction lengths), *i.e.* $\sigma_{had}(E) \approx (0.45 - 0.50) \cdot \sqrt{E}$. Our present purpose is to expose the effect of different amounts of passive material on the observable energy signal and resolution. This is appropriately done with our detector model using identical active calorimetry in all cases and regions.

There are three basic elements in the geometric setup used for the present study:

— A barrel calorimeter of the Argonne uranium-scintillator type as investigated[9] until the middle of 1990. For the current purposes, we give the model 38 towers of transverse dimensions of $\approx 10 \cdot 10\ cm^2$ at right angles to the beam and three more pointing to $z = \pm 380\ cm$ on either end, counting from the center in either direction along the beam. (The original model used[6] $3\frac{1}{2}$ towers at right angles and from there out to just above $z = \pm 4\ m$ towers of the same *projective* size pointing to $z = \pm 35\ cm$.) The ends of the barrel are covered with an aluminium cone; there is no cover on the front facing the beam axis. The aluminium cones are "abused" in the present study to include the front cover of the endcaps which the programmed model[6] does not contain as a separate volume element.

— An endcap calorimeter made of horizontally oriented towers of $10 \cdot 10\ cm^2$ size[6,9] , using the same uranium-scintillator material as in the barrel. It is positioned to appropriately reproduce the distances between the sensitive regions of the barrel and endcap. There is no passive cover material on the endcaps.

— A solenoid coil, made of three aluminium cylinders and aluminium end rings. The dimensions follow the current unified magnet design from Fermilab,[10] where we abuse the thickness of the outer cylinder to include a representation of the front cover of the barrel calorimeter. The two thin inner cylinders of the coil vessel are lumped together into one cylinder in our model. The winding is taken all the way out to the rings closing up the end. For the outer cylinder, the grid of ribs providing the mechanical rigidity is converted into an increased average cylinder thickness over the actual cylindrical shell as specified by R.Fast.[10]

The particular choice of the tower geometry in the barrel creates almost vertical cracks between the barrel and the endcaps as we need them for modelling the

current calorimeter designs. The cover material of the tile-fiber calorimeter is stainless steel; we have to convert this to an equivalent amount of aluminium as the simulation program[6] does offer only aluminium as a material to work with. The conversion is made by scaling the thicknesses up with the ratio of 2.66 of minimum-ionization energy losses in units of MeV/cm in order to maintain the correct energy loss in the absorbing material. For comparison, the ratio of radiation lengths is 5.06, the ratio of interaction lengths is 2.35, and the ratio of densities is 3.32, all quoted for applying them to scale the steel thickness up to an equivalent aluminium thickness. Our choice of the ratio of minimum ionization energies has been found to be appropriate by P.K.Job and J.Proudfoot in a study of the energy resolution and e/h ratio estimation of scintillator plate calorimeters.[11] Thus, we obtain the following thicknesses for passive material in the two models (we include the actual stell shell thicknesses for easy reference):

passive element	liquid argon	tile-fiber	tile-fiber, steel shell
coil inner cylinder	1.20 cm	1.20 cm	
coil central cylinder	7.80 cm	7.80 cm	
coil outer cylinder	7.50 cm	1.39 cm	0.32 cm
coil end rings	1.90 cm	1.90 cm	
barrel end cone	17.00 cm	6.77 cm	2.54 cm
air gap barrel-endcap	50 cm	7 cm	

The resulting geometries as seen by the simulation program are shown in Fig.1 (a complete 4π setup is used, not just the quadrant actually drawn in the figures).

To speed up the simulation process, we use a variant[12] of the bootstrap approach developed by E.Longo and L.Luminari[13] for the BGO calorimeter of the L3 experiment. The bootstrap showers have been created for a ZEUS style sampling of 3.3 mm uranium and 2.6 mm scintillator at four energies per decade from 10 MeV upward for electrons and pions. They are used in the present study for showers of 5 GeV or less from electrons, positrons and charged pions; all other particles are propagated in analog mode. We have included a protection against developing showers by this method near edges of the calorimeter where

a fraction of the shower might actually leak out of the sensitive region; in those places we let the program stick to the tedious analog particle-by-particle shower propagation. The integration time is set to 100 ns starting with the departure of the beam particle from the interaction point. Particles are followed down to kinetic energies of 100 keV except for photons which are taken down to 10 keV. The bootstrap showers have been created with the same cuts. Point deposits of energy created during the analog shower propagation are smeared with Poisson distributions with a variance of $0.15^2\ GeV^{-1} \cdot E_{deposit}$ to give the overall simulation a consistent resolution behavior. The choice of a Poisson distribution avoids the large negative tail of the smeared distribution of deposited energy which appear for a Gaussian of the same variance at the small energies of the deposits we have to deal with; the accumulated distributions for showers in the GeV energy range receive proper Gaussian-like shapes in this approach. The setups and simulation procedure as described here project out purely the effect of the passive material without the added complication of the differences in the response behavior of the active calorimeter regions of the two designs.

3. Analysis and results

We choose seven polar angles, 90°, 35°, 30°, 27°, 25°, 20° and 15°, to send negatively charged pions of 10 GeV/c momentum from the interaction point into each of the two setups described above (Fig.2). This particular momentum value is somewhat above the average of particle momenta of 6 GeV/c from interactions at the SSC, and is an important value also for triggering on jets for which thresholds in just the same order of magnitude will be used. At each angle, we accumulate the responses of the complete calorimeter, without pedestal subtraction or clustering, event-by-event for 500 events and fit single Gaussians to resulting distributions (Fig.3). From the fitted distributions, we find the mean response and the hadronic resolution of the setup at different polar angles. At the smallest angles, the tile-fiber model does not contain any passive material

in front of the sensitive region of the calorimeter; there the responses can be taken as reference points for measuring the effect of the passive material. (In the liquid-argon model, the edge of the barrel support cone reaches far enough down to still affect the response.) We observe that the mean response of the liquid-argon model is nearly twice as much reduced as the response of the tile-fiber model (Fig.4). The absolute loss of about one fifth of the signal in the worst case is not desastrous, the distribution is still Gaussian (Fig.3). Much more serious is the loss of resolution which increases by almost two thirds over the value without any passive material in the liquid-argon case and by one half in the tile-fiber case (Fig.5). The deterioration becomes even more evident when we determine at each angle the coefficient c in the resolution law $\sigma/E = c/\sqrt{E_\pi}$ as we show in Fig.6, here the liquid-argon model shows twice the amount of deterioration as compared to the tile-fiber model. While the mean response can be compensated for by using an angle-dependent calibration, any improvement in the resolution has to be accomplished by changing the design of the whole setup.

4. Summary

We have studied the effect of passive materials used to build vessels closing up the calorimeter for the SDC detector by simulation the calorimeter response to negatively charged pions of 10 GeV/c momentum. Our simulation has identical calorimetry behind the models of passive materials representing the current designs for a tile-fiber calorimeter and a liquid-argon calorimeter, representing the response of either option appropriately while avoiding any uncertainty due to differences in detail of the behaviour of the active calorimetry. The deterioration of the response in the liquid-argon case is much worse than in the tile-fiber case. This result strongly favors the choice of the tile-fiber design.

ACKNOWLEDGEMENTS

We would like to thank Dr. James Proudfoot for suggestions, comments and continued interest throughout the development of the present study.

REFERENCES

1) Solenoid Detector Collaboration, G.H.Trilling et al., SDC-90-00085 and SSC-EOI-3, SSC Laboratory, Dallas, Texas, May 24, 1990, and SDC-90-00151 and SSC-LOI-1, SSC Laboratory, Dallas, Texas, November 30, 1990

2) A.M.Jonckheere, Simulating D0 and Hermeticity Studies or How to Effect a Detector Design, Proc. Workshop on Detector Simulation for the SSC, August 24-28, 1987, ed. L.E.Price, ANL-HEP-CP-88-51, Argonne National Laboratory, Argonne, Illinois, USA 1988, p.270, p.175

3) M.Strovink, W.J.Womersley and G.E.Forden, Hermeticity of three Cryogenic Calorimeter Geometries, Proceedings of the Workshop on Calorimetry for the Supercollider, March 13-17, 1989, Tuscaloosa, Alabama, U.S.A., eds. R.Donaldson and M.D.G.Gilchriese, World Scientific Publishing Co. Pte. Ltd., Singapore, 1990, p.9

4) R.Ruchti, Summary Report for the Scintillating Fiber Working Group, Proceedings of the Workshop on Tracking Systems for the Superconducting Supercollider, July 24-28, 1989, TRIUMF Laboratory, Vancouver, Canada, 1989, E3

5) R.E.Blair, L.E.Price and H.-J.Trost, program ANLSIM, Argonne National Laboratory, Argonne, Illinois, USA 1989, version 1.05, 1991 (unpublished);
H.-J.Trost, ANLSIM, talk given at: Workshop on the Future Development of GEANT, SSC Laboratory, Dallas, Texas, Jan.10-13, 1990, unpublished;
R.E.Blair, The Argonne National Laboratory Simulation Package, Proceedings of the Workshop of Physics and Detector Simulation for SSC Experiments, SSC Laboratory, Dallas, Texas, January 9-19, 1990, vol.1, p.69;
H.-J.Trost, How to Use ANLSIM, ibid., vol.2, p.265

6) J.Proudfoot and H.-J.Trost, A first simulation study of the barrel-endcap transition region in a calorimeter of the scintillator tile design, ANL-HEP-TR-90-77 and SDC-90-00073

7) E.Bernardi *et al.*, Nucl.Instr.Meth. A262 (1987) 229

8) W.Braunschweig *et al.*, Nucl.Instr.Meth. A265 (1988) 419;
W.Braunschweig *et al.*, Nucl.Instr.Meth. A275 (1989) 246;
H1 Calorimeter Group, W.Braunschweig *et al.*, internal report DESY 89-022, Deutsches Elektronen-Synchrotron, Hamburg, Germany, 1989

9) N.Hill, Observations and conclusions drawn from conceptual design exercises on barrel calorimeter for SDC, internal note, Argonne National Laboratory, May 30, 1990 (unpublished)

10) R.Fast *et al.*, SDC Calorimeter Group Meeting at Fermilab, May 21-22, 1991

11) P.K.Job and J.Proudfoot, Estimation of Hadronic and EM Resolution for Scintillator Plate Calorimeter Configurations, ANL/HEP/TR-91/11 and SDC-91-00013

12) H.-J.Trost, The bootstrap method for simulation of showers in sampling calorimeters, note in preparation

13) E.Longo and L.Luminari, Fast electromagnetic shower simulation, Nucl. Instr.Meth. A239 (1985) 506

FIGURE CAPTIONS

1. GEANT geomentries for a) the tile-fiber setup and b) the liquid-argon setup

2. Example of a single π^- of 10 GeV/c momentum propagated through a) the tile-fiber setup, b) the liquid-argon setup at a polar angle of 27°. Particle traces for kinetic energies above 10 MeV (this is higher than the simulation cuts used) are shown.

3. Examples of the observed energy distribution with a Gaussian fit for a) 90° and b) 27° in the tile-fiber setup, and c) 90° and d) 27° in the liquid-argon setup.

4. Mean response as a function of polar angle.

5. Resolution for π^- at 10 GeV/c momentum as a function of polar angle.

6. Resolution coefficient c for $\sigma/E = c/\sqrt{E_\pi}$ as a function of polar angle.

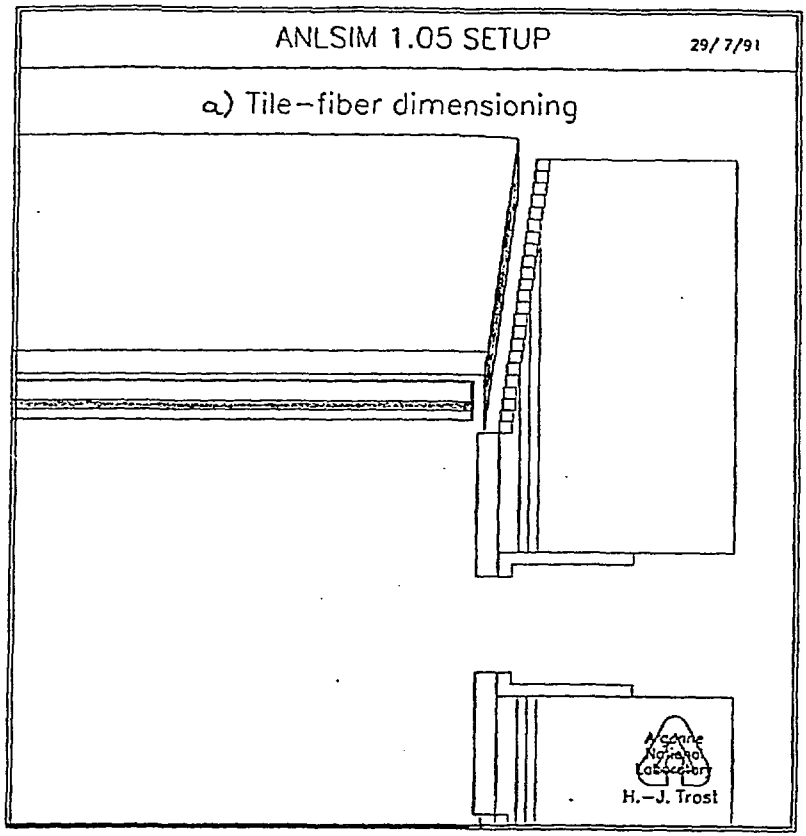
ANLSIM 1.05 SETUP
29/7/91
a) Tile-fiber dimensioning
H.-J. Trost

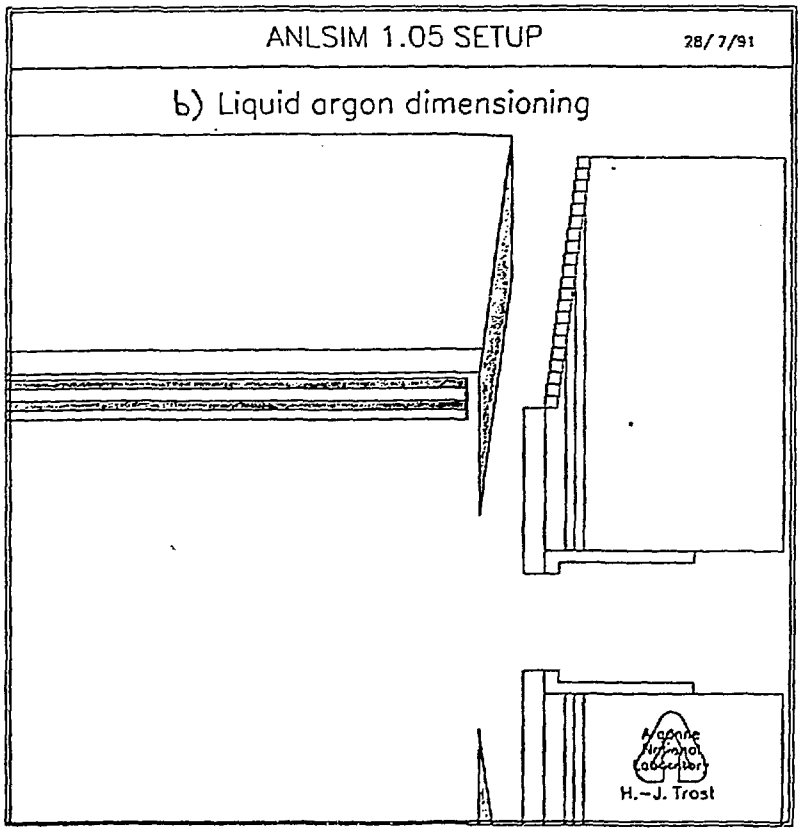
ANLSIM 1.05 SETUP
28/7/91
b) Liquid argon dimensioning
H.-J. Trost

Fig. 1

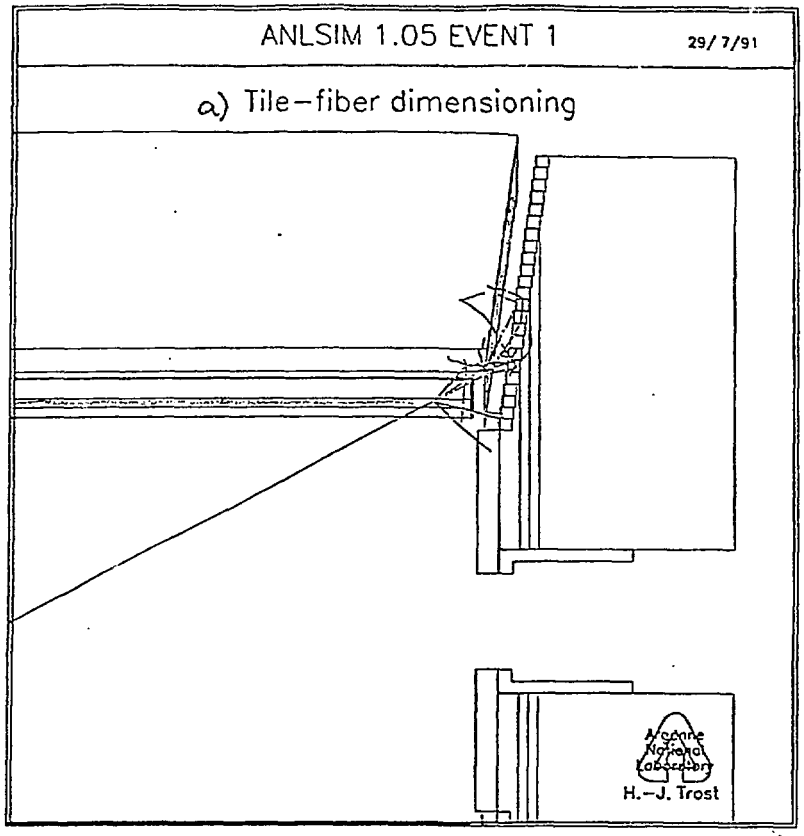
ANLSIM 1.05 EVENT 1
29/ 7/91
a) Tile–fiber dimensioning
Argonne National Laboratory
H.–J. Trost

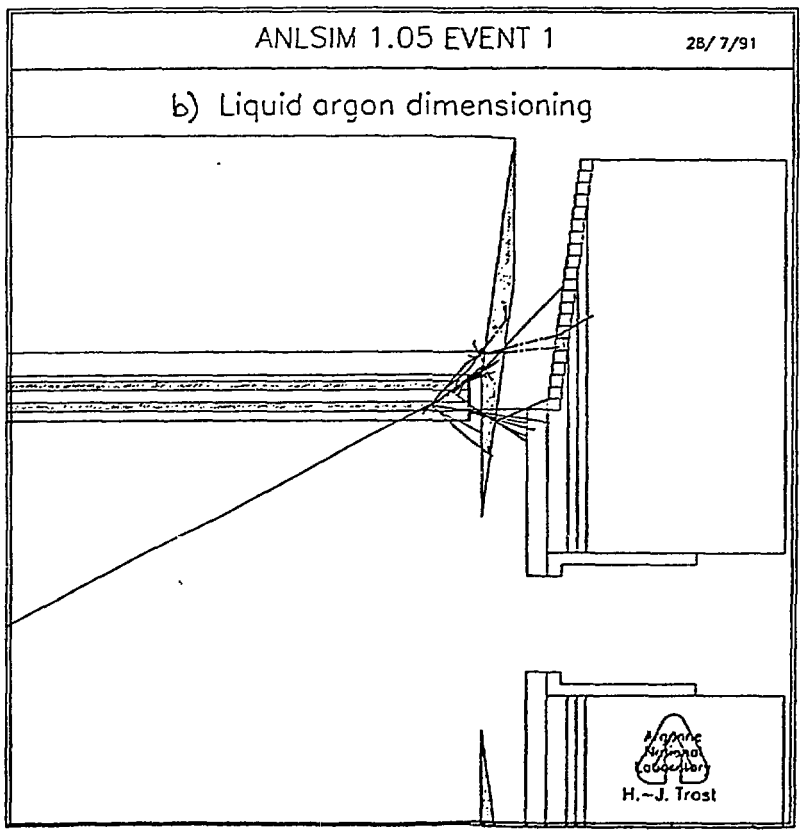
ANLSIM 1.05 EVENT 1
28/ 7/91
b) Liquid argon dimensioning
Argonne National Laboratory
H.–J. Trost

Fig. 2

06/08/91 08.56

Examples of fitted response distributions

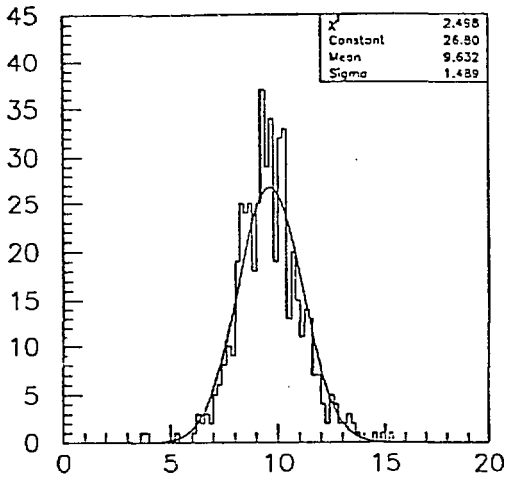

a) Tile–fiber model at 90°

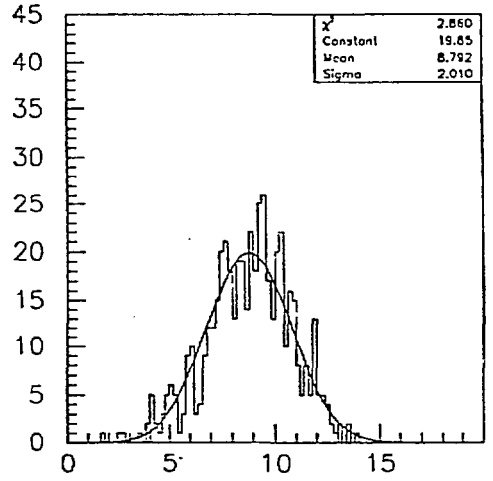

b) Tile–fiber model at 27°

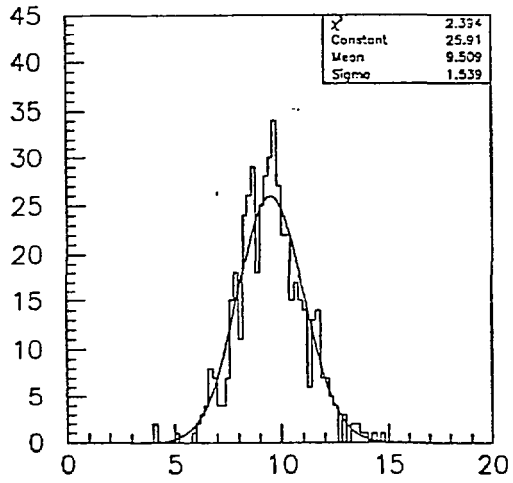

c) Liquid–argon model at 90°

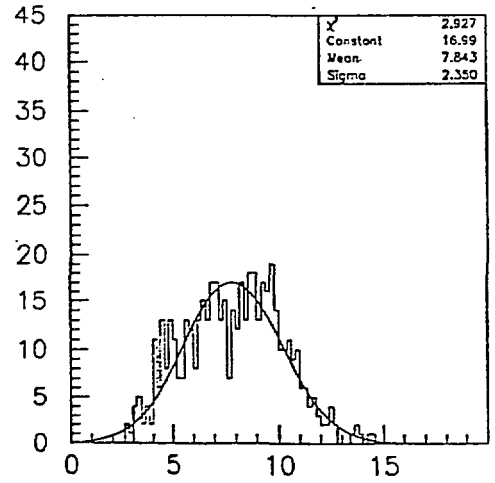

d) Liquid–argon model at 27°

Fig. 3

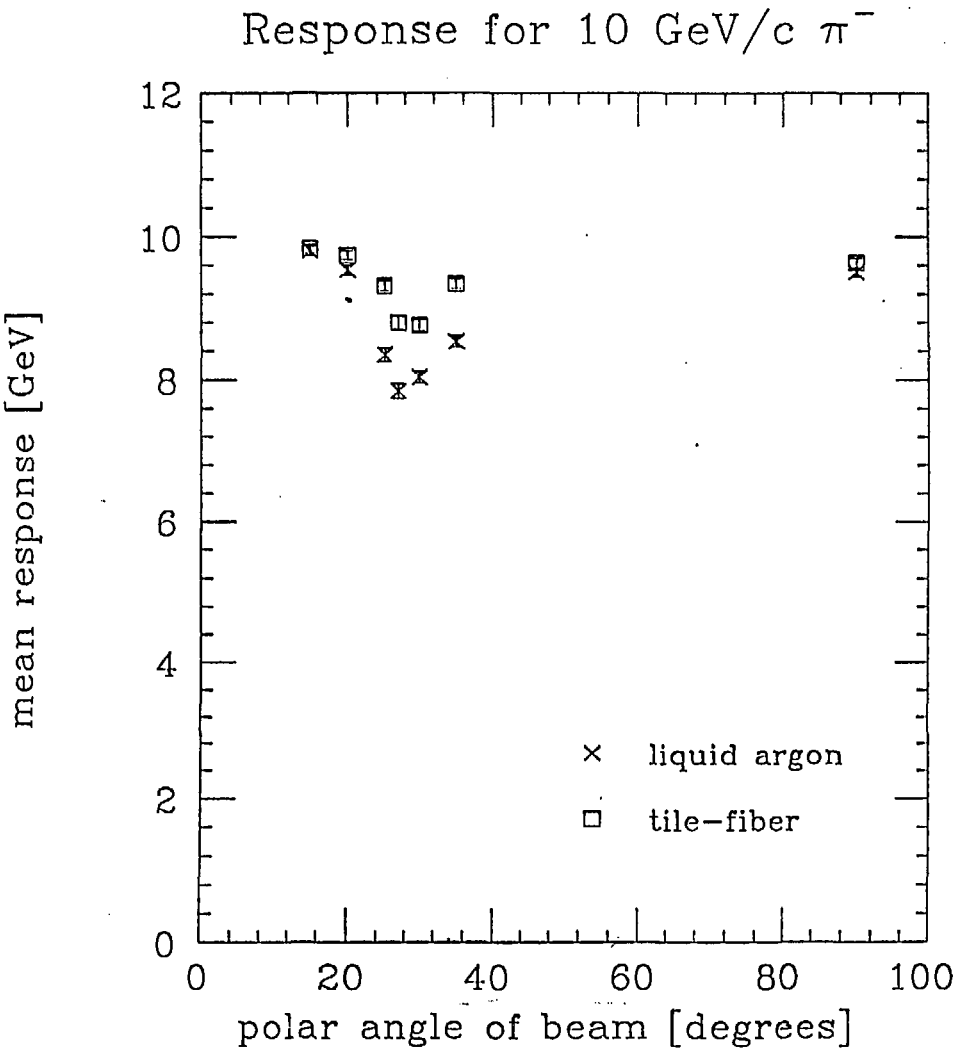
Response for 10 GeV/c π^-
mean response [GeV]
polar angle of beam [degrees]
liquid argon
tile–fiber
0
2
4
6
8
10
12
0
20
40
60
80
100

Fig. 4

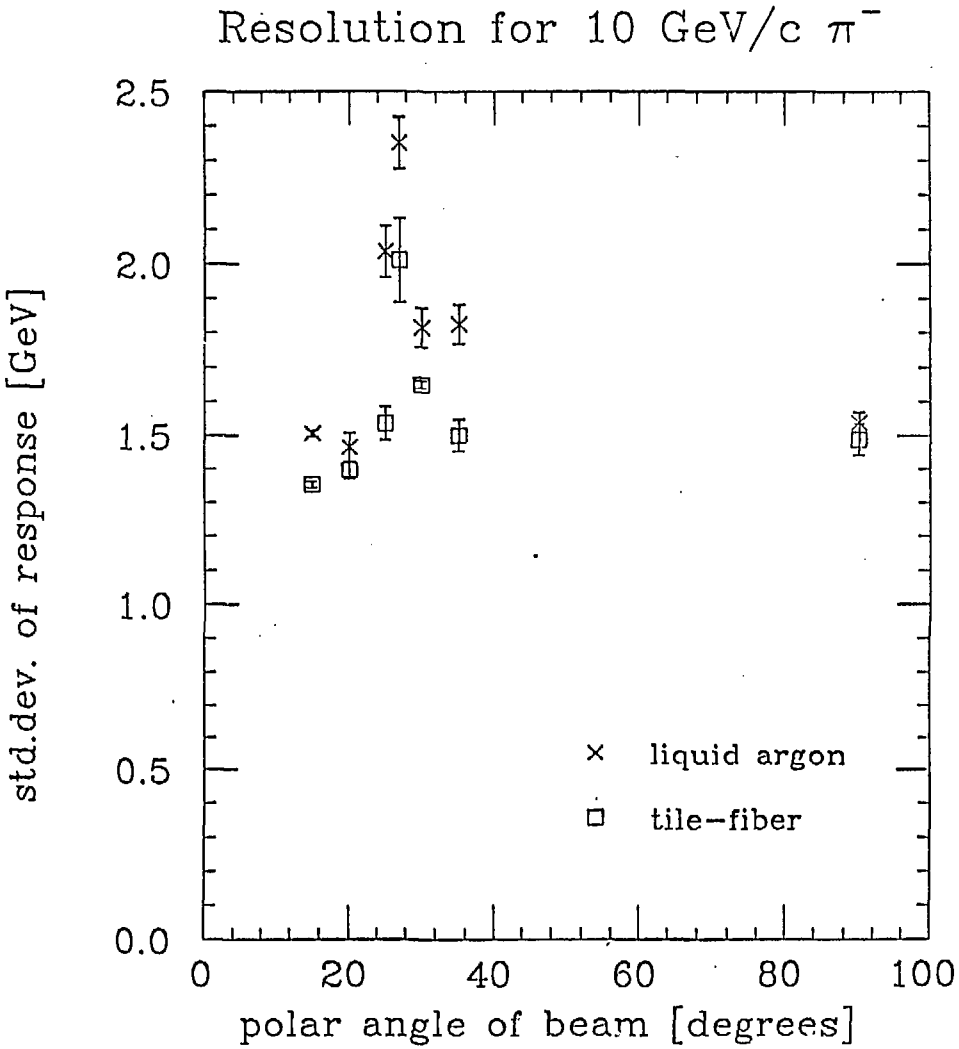
Resolution for 10 GeV/c π^-
std.dev. of response [GeV]
2.5
2.0
1.5
1.0
0.5
0.0
0
20
40
60
80
100
polar angle of beam [degrees]
liquid argon
tile–fiber

Fig. 5

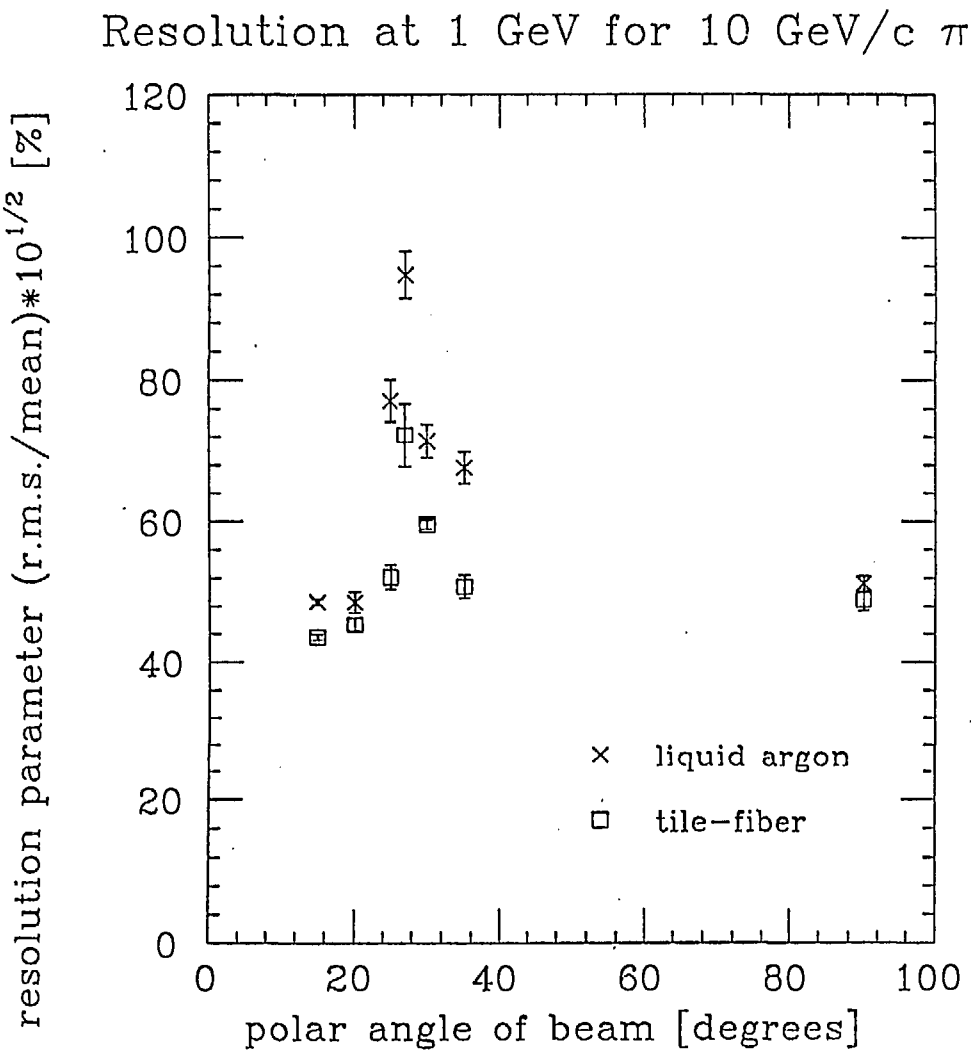
Resolution at 1 GeV for 10 GeV/c π^-
resolution parameter (r.m.s./mean)*$10^{1/2}$ [%]
polar angle of beam [degrees]
liquid argon
tile–fiber
0
20
40
60
80
100
120

Fig. 6